An Engineering Analysis of Crack Growth at Transverse Stiffeners

Une analyse technique de l'accroissement de fissures aux raidisseurs transversaux

Eine technische Berechnung der Ausbreitung von Rissen an Querversteifungen

P. ALBRECHT
Asst. Prof. of Civil Engr., University of Maryland; former Research Asst., Fritz Engineering Lab., Lehigh University

J.W. FISHER
Prof. of Civil Engr., Assoc. Director, Fritz Engr. Laboratory, Lehigh University, Bethlehem, Pa.

Introduction

In this paper the fatigue behavior of welded beams and girders with transverse stiffeners is described.

Further, it is shown that for purposes of design, the constant amplitude fatigue life of stiffener details often encountered in highway bridge construction can be predicted using fracture mechanics concepts of crack propagation. To accomplish this, the stress intensity factor is estimated and the analysis is performed assuming that the portion of the life expended during initiation is negligible when compared with the number of cycles required to propagate the crack. Such an assumption appears to be justified for details having a high notch effect, and which are susceptible to initial flaws built-in during the fabrication process.

In general, initiation and growth of fatigue cracks are most likely to occur in areas subjected to a high tensile stress range and where initial flaws exist. The higher the stress range and the larger the initial flaw, the faster fatigue cracks will propagate. Both conditions exist along the toe of the fillet welds connecting the stiffeners to the web or flanges.

The initial flaw condition is given by discontinuities at the weld toe, such as weld cracking, slag inclusions and undercut [3, 5]. Imperfections of this nature are common to all welding processes. They cannot be avoided, although their sizes and frequency of occurrence may be controlled by good welding techniques.

Secondly, the critical tensile stress range which drives the crack is brought about by a combination of two effects. One is the geometrical stress concentration produced by the weld geometry and the stiffener which magnify the stresses due to the applied loads. Further, a residual tensile stress field is generated by the welding process. The net effect of having residual tensile stresses and the stresses due to the applied load is a tension-tension stress range at the weld toe, even in cases of nominal stress reversal. In fact, fatigue cracks were also observed at weld toes sub-

jected to a nominal compression-compression stress cycle. These cracks, however, arrested as they outgrew the residual tension field and did not impair the load carrying capability of the beam.

Experimental Investigation

The experimental investigation consisted of testing thirty 14-inch (168 mm) deep beams and twenty-two 38-inch (965 mm) deep girders. All specimens had stiffeners welded to the web, as well as stiffeners welded to the web and flanges. The stiffeners were located in a region of moment gradient as shown in Fig. 1.

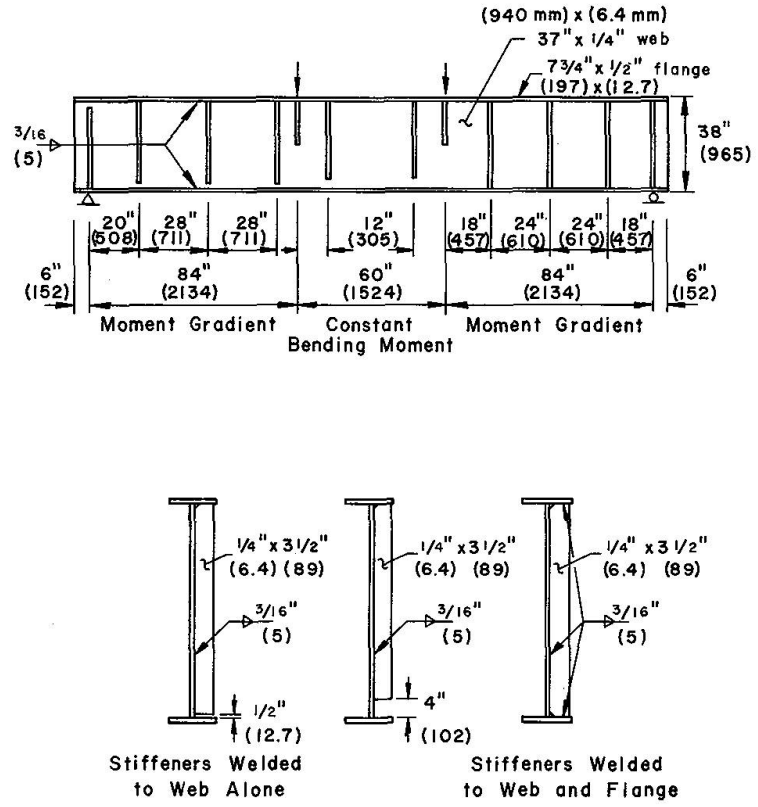

Fig. 1. Details of Test Girders.

To permit the statistical evaluation of the significance of several stress and geometrical variables, the specimens were arranged into factorial experiments. The experimental data including an analysis of the test variables were presented in Refs. 1 and 2. It was found that the bending stress range is the dominant variable which defines the fatigue strength of full depth transverse stiffener details. Other variables such as maximum stress, specimen size, yield strength, and type of stiffener (welded to the web alone or to the web and flanges), are not significant for purposes of design of stiffened bridge members.

Crack Initiation and Growth

Fatigue cracks at the stiffeners, whether welded to the web alone or welded to the web and flanges, had one major feature in common: the cracks initiated and grew from surface flaws at the toe of non-load carrying fillet welds. Also, the plane of the crack remained at all stages perpendicular to the direction of the principal stress.

Stiffeners Welded to the Web and Flanges

A typical fatigue crack causing failure at a stiffener welded to the web and the flanges is shown in Fig. 2. Crack growth was characterized by the two stages illustrated in Fig. 3. During the first stage, one or more cracks initiated along the toe of the fillet weld connecting the stiffener to the tension flange, and propagated in a semi-elliptical shape as shown in Fig. 4. When the small cracks grew larger they joined and eventually assumed the shape of a larger semi-elliptical crack as illustrated in Fig. 5. By the time the leading edge reached the extreme fiber of the tension flange, the crack width had spread over most of the weld length. After breaking through the extreme fiber, it grew in the second stage as a through crack across the tension flange and up into the web. Visual observation of several specimens indicated that approximately 96% of the number of cycles to failure

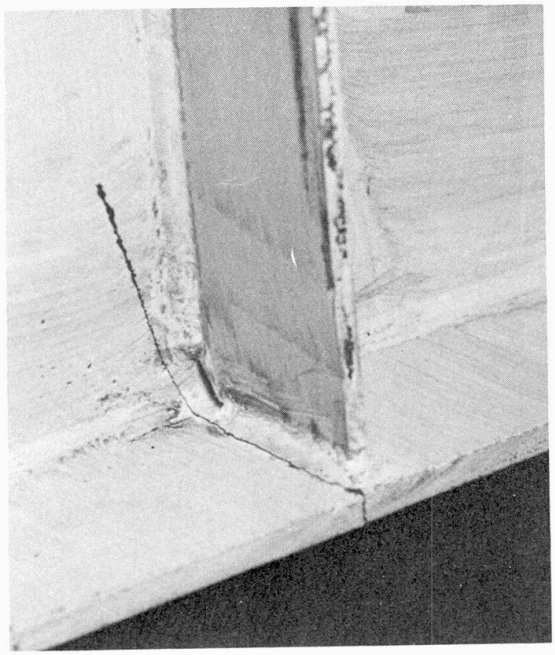

Fig. 2. Typical Failure at Stiffeners Welded to Web and Flange.

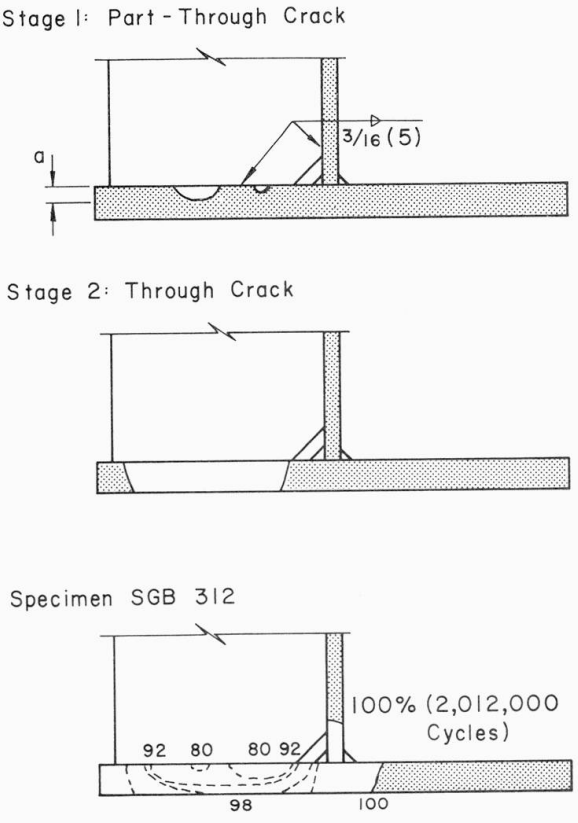

Fig. 3. Stages of Crack Growth at Stiffener-to-Flange Connection.

Fig. 4. 0.028-inch Deep Crack at the Toe of the Stiffener-to-Tension Flange Weld.

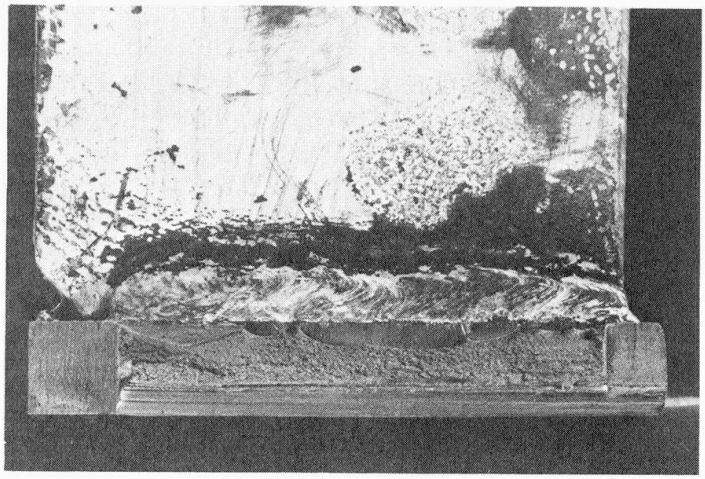

Fig. 5. Multiple Fatigue Crack Growth at the Toe of Stiffener-to-Tension Flange Weld.

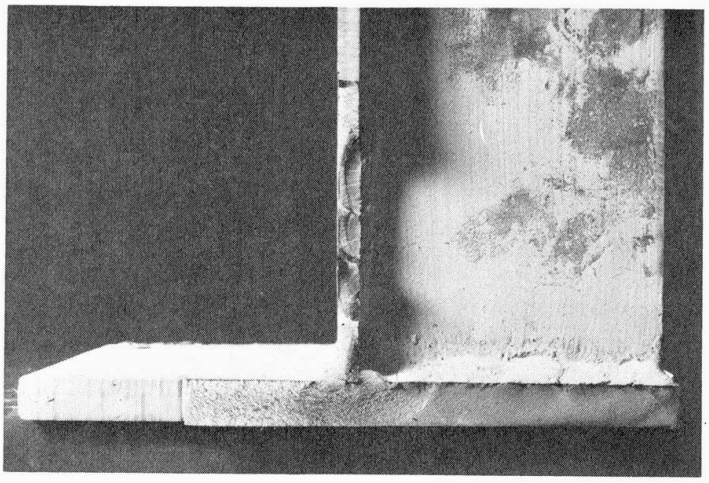

Fig. 6. Typical Fatigue Crack Surface at Failure.

were consumed growing the crack through the thickness of the flange. The remaining 4% of the life was spent in Stage 2 of growth. Figure 3 illustrates the extent of crack growth observed on the surface of the flange plate at different numbers of applied cycles. The contour and depth of the leading edge of the part-through at 80% and 92% of the final life are shown qualitatively.

Figure 6 shows a fatigue crack surface at failure. The crack is seen to have initiated at the stiffener-to-flange weld. As it eventually advanced up into the web, it joined with several semi-elliptical cracks growing from the toe of the stiffener-to-web weld.

Stiffeners Welded to the Web Alone

The cracks causing failure at the stiffeners welded to the web alone initiated at one or more points along the toe of the stiffener-to-web weld. They propagated in a direction perpendicular to the principal tensile stress.

The overall appearance of the crack seemed to indicate two growth patterns, one diagonally off the end of the stiffener-to-web weld, the other following the weld toe before branching off diagonally into the web as illustrated in Fig. 7. The fatigue crack surfaces were exposed by saw cutting most of the net section and prying the remaining ligaments open. This fractographic examination revealed the reasons for the two observed patterns. Cracks initiating at the end of the weld (at one point), grew in all stages along a plane perpendicular to the changing direction of the principal stress as illustrated in Fig. 8. Cracks following the weld toe had multiple initiation points from which individual cracks grew in separate planes, each one perpendicular to the direction of the principal stress at that point. As the individual cracks overlapped they broke through and joined each other, forming a longer crack with an irregular contour along the weld toe as illustrated in Fig. 9b. This phenomena gave the appearance of a crack growing along the toe of the weld,

Fig. 7. Typical Failure at Web Stiffeners.

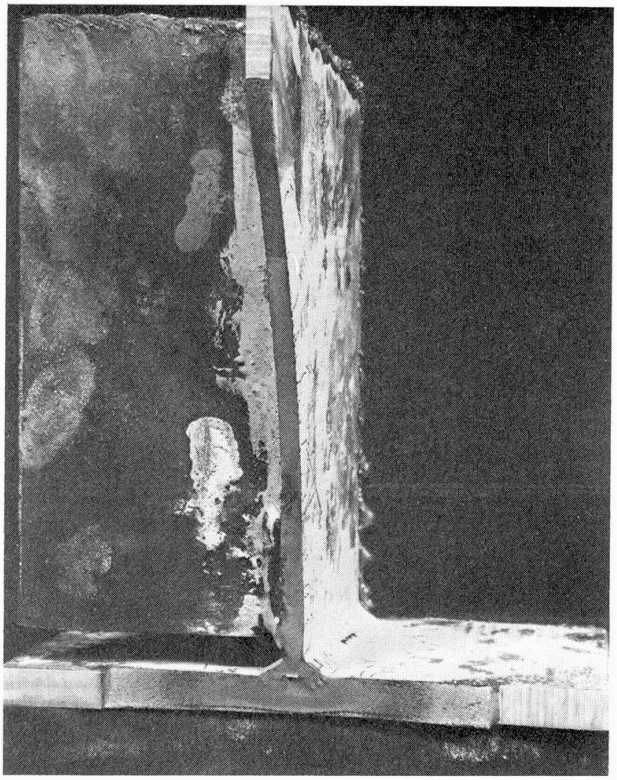

Fig. 8. Typical Fatigue Crack Surface at Web Stiffener at Failure.

before branching off diagonally. Once this pattern had developed it was sustained by the stress concentration effect of the weld which created a more severe path for propagation along the toe than in the web away from the weld toe.

Typically, the crack advanced through the three stages of growth as depicted by Fig. 10. In the first stage, one or more semielliptical cracks were driven through the thickness of the web plate, as shown in Fig. 9. Each one retained the approximate shape of a semiellipse as long as it did not join and interact with adjacent cracks.

Once the crack front had penetrated the web plate, the crack changed into a two-ended through crack. This transition after web plate penetration into Stage 2 occurred within a short number of cycles. Figures 9c shows one part-through crack at the beginning of the transition and one at the end.

In the third stage, after the lower front of the two-ended crack had broken through the extreme fiber of the tension flange, it grew as a three-ended crack (see Figs. 8 and 10) across the flange and extended further up into the web. Eventually, the ever decreasing net section of the flange yielded, and the test was terminated before the flange fractured. No "brittle" fracture was observed in any of the specimens.

Of the total number of cycles to failure at web stiffeners, 80% were consumed growing the crack through the thickness of the web plate during Stage 1. The second and third stages amounted to 16% and 4% respectively as indicated schematically in Fig. 10.

Figure 9 shows small ellipses inside the fatigue crack surface. They correspond to the crack size at the time the beam had failed at stiffeners welded to the web and flange and reflect the oxidation of the crack area.

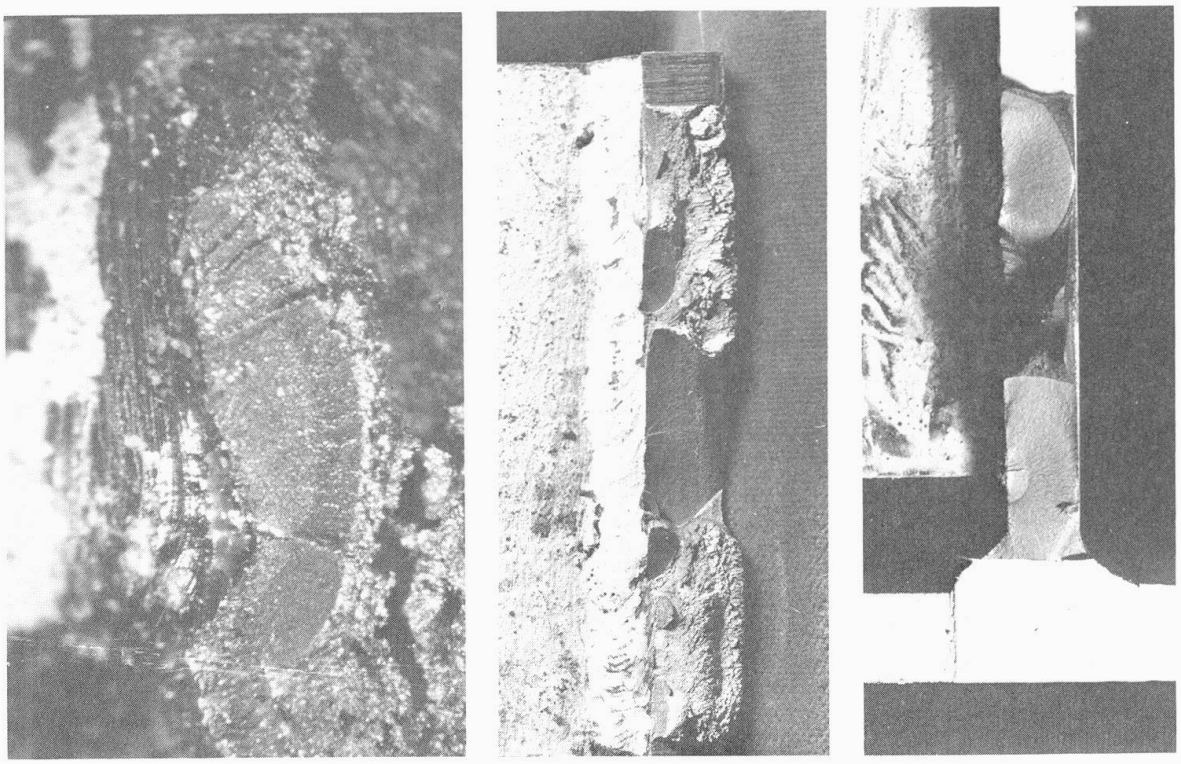

(a) 0.035-inch Deep Crack. (b) Multiple Fatigue Cracks. (c) Multiple Fatigue Cracks through the Web.

Fig. 9. Fatigue Crack Growth at the Toe of Stiffener-to-Web Weld.

Mathematical Model for Crack Propagation

The fatigue life of a detail is defined by the sum of the number of cycles required for crack initiation and the number of cycles required for crack propagation to failure. Available information indicates that the fatigue life prediction of welded details can be based on crack propagation alone [1, 4, 5]. In this study fatigue life was estimated by considering crack propagation alone and any initiation phase was ignored.

SIGNES et al. [3] showed that fatigue cracks initiate at the toes of fillet welds from mechanical defects constituting a sharp notch with a typical root radius of 0.0001 inch (0.0025 mm) or less when the applied stress was perpendicular to the weld toe. These crack-like defects exist in welds made with all conventional welding processes. They are equivalent to an initial crack, which propagates under repeated loading. WATKINSON et al. [5] reported directly comparable fatigue lives for welded joints in an as-welded condition and welded joints with an additional machined

notch with a depth of 0.005 inch (0.127 mm) and 0.0005 inch (0.013 mm) root radius. Since the added notch did not lead to a further reduction in fatigue strength, it was assumed that the sharp weld defects constituted an equally severe initial crack condition and that fatigue life prediction of welded joints can be based on crack propagation alone.

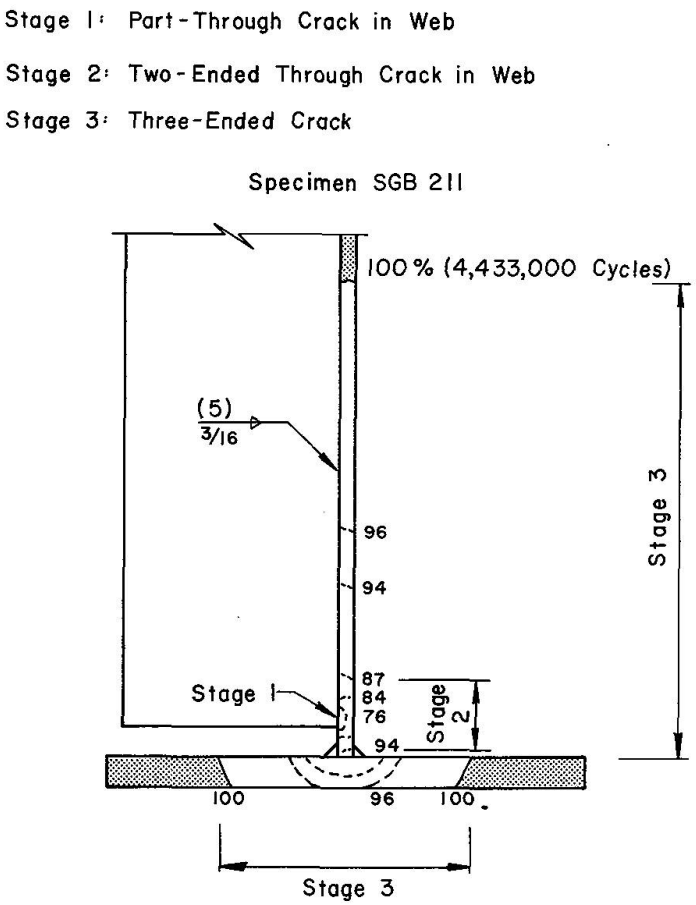

Fig. 10. Stages of Crack Growth at Web Stiffeners.

Analysis of Crack Propagation

The fracture mechanics approach to crack propagation appears to be the most rational method currently available for predicting the fatigue life. It has been used to provide an explanation of the fatigue crack growth of a number of welded steel details.

The empirical differential equation of crack growth proposed by Paris [6] has the form:

$$\frac{da}{dN} = C\,(\Delta K)^n \tag{1}$$

and relates measured rates of crack growth (da/dN) to ΔK, the range of the stress-intensity factor K proposed by IRWIN [7]. C and n are constants. Equation 1 can be integrated to obtain the number of cycles N required to propagate a crack

from an initial size a_i to a final size a_f. For stress ranges of constant amplitude and assuming that C and n remain constant within the span of ΔK values which are of major importance, the integration yields:

$$N = \frac{1}{C} \int_{a_i}^{a_f} \frac{1}{(\Delta K)^n} da = \frac{\sigma_r^{-n}}{C} \int_{a_i}^{a_f} \frac{da}{(\Delta K/\sigma_r)^n} \tag{2}$$

As was noted in Ref. 8, Eq. 2 suggests that the relationship between the Life N and the applied stress range σ_r is exponential and can be expressed as:

$$N = G\, \sigma_r^{-n} \tag{3}$$

where

$$G = \frac{1}{C} \int_{a_i}^{a_f} \frac{da}{(\Delta K/\sigma_r)^n} \tag{4}$$

Since ΔK, the range of the stress intensity factor, is directly proportional to the applied stress range σ_r, G is independent of σ_r. The results of an extensive statistical analysis of fatigue data collected from over 500 full size beam specimens [1] [8] bears out the validity of the above conclusions for purposes of fatigue design of structural details built from steels commonly used in highway bridge construction. Indeed, of all models investigated, the linear regression equation

$$\log N = B_1 - B_2 \log \sigma_r \tag{5}$$

provided the best fit to the experimental data. From Eqs. 3 and 5 it is also apparent that B_2 and n are the same.

The solution of Eq. 2 requires a knowledge of the constants C and n, and an adequate approximation for the stress intensity factor for the crack at the detail being examined.

Crack Growth Rates

The coefficient C and the exponent n in Eq. 1 are constants which define the rate of crack growth for a given value of ΔK. They are determined empirically from tests of precracked "fracture mechanics" specimens for which an analytical expression for the stress intensity factor, ΔK, is known. From measurements of crack size, the increases in size corresponding to increments of cyclic loading are related to the range of the stress-intensity factor, ΔK.

Several investigators have reported growth rates for structural steels [9, 10, 11, 12]. BARSOM [9] found that the growth rates in four ferrite-pearlite steels fell into a band. He suggested that the slope of the logarithmically transformed data decreased slightly as the yield strength increased. The slope varied from 3.3 to 2.8 for steels with yield strengths between 36 (25) and 69 ksi (48 kN/mm^2). Data have also been reported by CROOKER and LANGE [11]. A relatively large scatterband was indicated for carbon and low-alloy determined the growth rates for four different weld metals. Three of the weld metals had yield strengths equal to about 67 ksi (46 kN/mm^2) and the fourth to 90 ksi (62 kN/mm^2).

Most of the test data on crack growth is for ΔK values above 10 ksi $\sqrt{\text{in.}}$ (11 MP a$\sqrt{\text{m}}$). Only a limited amount of data is available below that level. PARIS [10] reported on very slow growth and suggested a threshold value at $\Delta K = 5$ ksi $\sqrt{\text{in.}}$ (5.5 MPa$\sqrt{\text{m}}$).

From a study of experimental results published in the literature, HARRISON [13] concluded that fatigue cracks will not propagate in mild steel if $\Delta K < 3.3$ ksi $\sqrt{\text{in.}}$ (3.6 MPa$\sqrt{\text{m}}$). The level of the threshold was observed to be also a function of the mean stress [10], the threshold being lower the higher the mean stress. Hence, a low threshold value can be expected for fatigue crack growth from weld toes where the applied stresses are magnified by the discontinuities of the weld geometry and where high residual tensile stresses are known to exist.

The coefficients of the crack growth equation were also established by HIRT and FISHER [14] using the equivalence between the crack growth equation and the stress range-cyclic life relationship for plain welded beams. A penny-shaped crack was assumed to describe the disc-like cracks that grew in the flange-to-web weldment of beams. This yielded values of $n \simeq 3$ and $C \simeq 2 \times 10^{-10}$ where C has the units implied by Eq. 1 assuming ΔK in units of ksi $\sqrt{\text{in}}$ and da/dN in units of inches. ($C \cong 3.8 \times 10^{-9}$ when ΔK in. MPa$\sqrt{\text{m}}$ and da/dN in millimeters).

In this study it was assumed that C and n remained constant for all values of ΔK. The relationship found by HIRT and FISHER was rounded and used. The crack growth rate was taken as

$$\frac{da}{dN} = 2 \times 10^{-10} \Delta K^3 \tag{6}$$

for all details. The relationship developed from beam test is in good agreement with the crack growth data from fracture mechanics specimens. The beam tests had indicated that crack initiation took place at values of ΔK between 3 (3.3) and 5 ksi $\sqrt{\text{in.}}$ (5.5 MPa$\sqrt{\text{m}}$). This was at or below the threshold level suggested by PARIS [10].

Stress-Intensity Factors for Part-Through Cracks at Fillet Weld Toes

With an appropriate expression for the stress-intensity factor K at the toe of a non-load carrying fillet weld, the propagation of a crack through the thickness of the web or flange can be predicted. As noted in the discussion of crack growth at stiffener details, 80% of the total number of cycles to failure for web stiffeners were consumed by crack propagation of a flaw through the thickness of the web and 96% for stiffeners welded to the flange. Hence, an analysis of this stage of fatigue crack growth represents essentially a study of the fatigue life of beams with stiffeners.

It was observed that cracks at both types of stiffeners initiated from discontinuities at the weld toe and propagated as a semi-elliptical crack through the thickness of the web or the flange plate during most of the specimen's life.

The average change in shape of crack size was found empirically. After the beam had failed at the critical stiffener the planes through the weld toes of the other less critical stiffeners were exposed. Subsequent examination of the surfaces, both visually and with a 50 × microscope, revealed the presence of part-through cracks at specific stages of growth in a large number of specimens [2]. The measured crack sizes are plotted in Fig. 11, together with the exponential relationship.

$$b = 1.088a^{0.946} \tag{7}$$

describing the average change in size, where b and a are the two semi-axes of the semi-elliptical crack. This variation of b with a was considered in the analysis of fatigue crack propagation. Equation 7 is seen to approach the circular crack ($a/b = 1$) with increasing crack size.

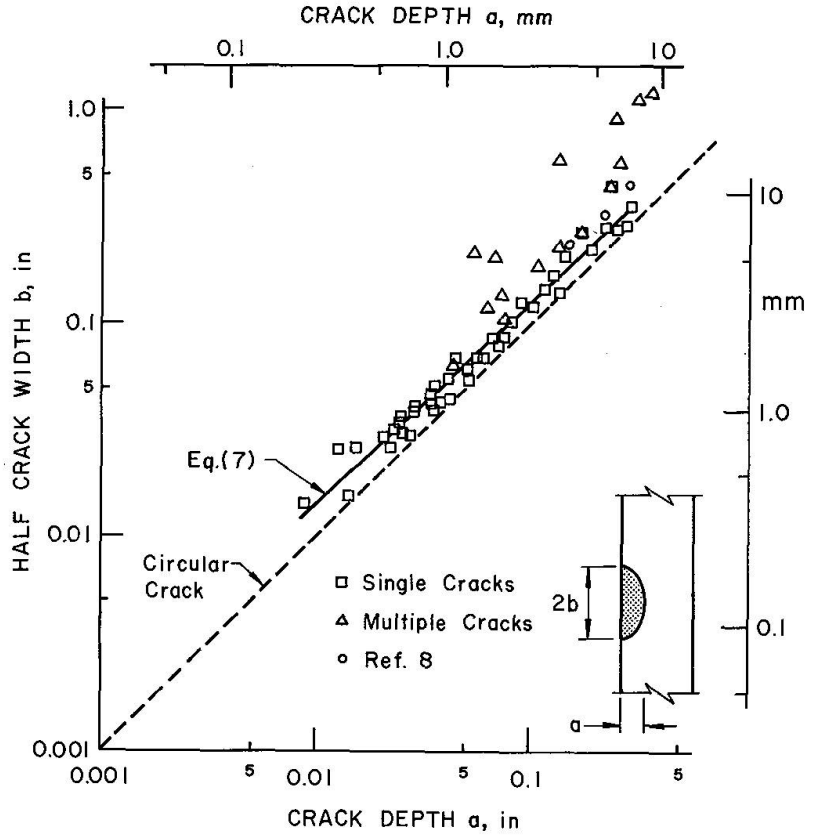

Fig. 11. Size of Part-Through Cracks at Fillet Weld Toes.

Part-through cracks which initiated at more than one point are also plotted in Fig. 11 as open triangles. They were not included in the regression of b on a. Three part-through cracks observed at the end of longitudinally welded cover plates [8] are shown as circles and fall near the mean regression line.

The stress-intensity factor for a part-through crack developed by IRWIN [16] can be used with the secant correction [17] for a free surface representing the side of

the plate opposite from the crack opening to describe the condition illustrated in Fig. 12a. This results in

$$K = \frac{1+0.12(1-a/b)}{\Phi_o} \sigma \sqrt{\pi a} \sqrt{\sec \frac{\pi a}{2t}} \tag{8}$$

where Φ_o is an elliptical integral which depends on the minor to major axis ratio, a/b, of the crack.

Equation 8 cannot be directly applied to part-through cracks at the toe of non-load carrying fillet welds connecting stiffeners to the flange and the web, unless the stress concentration effect of the weld is considered. If the part-through crack is removed from the uniformly stressed flat plate shown in Fig. 12a, then the stress field, σ, will remain constant throughout the plate. This is not the case for the detail shown in Fig. 12b which represents a plate strip of either the web or the flange with a portion of the stiffener welded on.

In the absence of a crack, the weld geometry acts as a stress raiser, magnifying the nominal stress at the weld toe by the stress concentration factor K_T. The stress concentration effect decays rapidly with increasing distance from the weld toe.

In order to apply the stress intensity factor given by Eq. 8 to the detail shown in Fig. 12b requires an additional geometry correction function accounting for the stress magnification effect of the weld. FRANK used a finite element and compliance analysis to evaluate the stress-intensity factor for tunnel-shaped cracks at

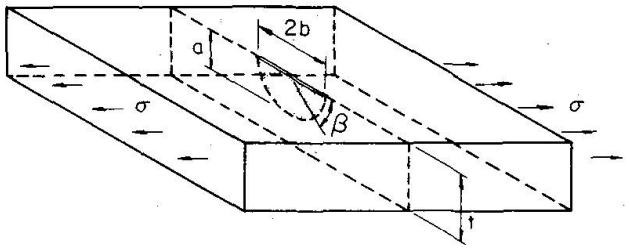

Fig. 12a. Part-through Crack in a Flat Plate.

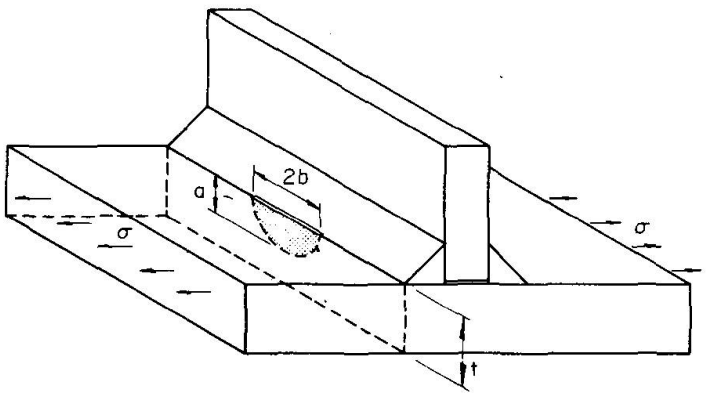

Fig. 12b. Part-through Crack at the Toe of a Non-load Carrying Fillet Weld.

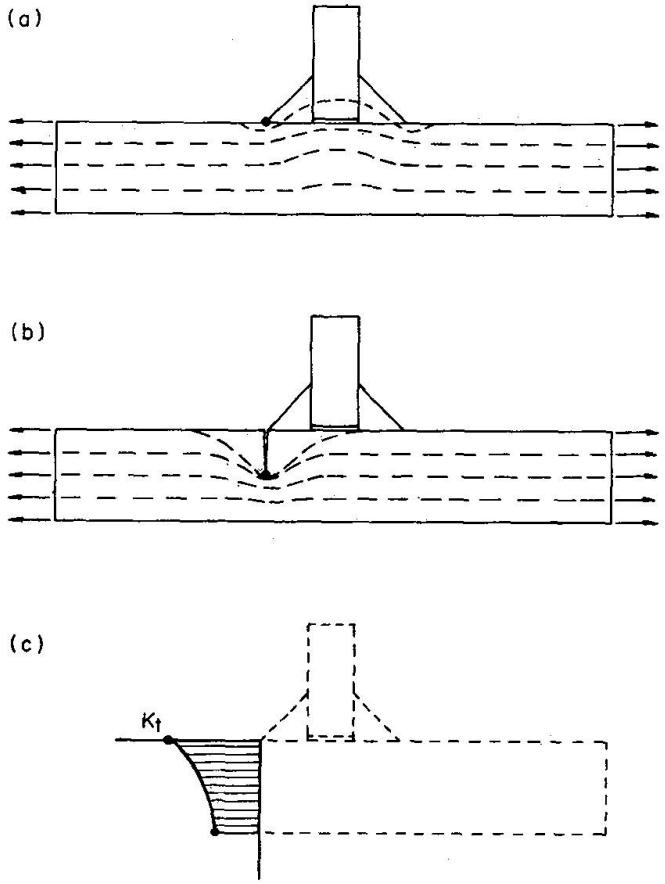

Fig. 13. Correction Function for the Applied Stress Field.

the weld toe of cruciform joints [4]. On the basis of this analysis he developed a correction function for the weld geometry which was equal to the stress concentration factor, K_T for vanishing crack size and which decreased as the crack propagates into the plate (see Eq. 9). Others have assumed a constant value of K_T for the correction function of a similar detail but did not make an allowance for the decay with increasing distance from the weld [19].

The idea of utilizing the theoretical stress concentration factor, K_T, to arrive at an estimate of the stress intensity factor, K, is not a new one. It is well known, for example, that K for a small crack emanating from a much larger circular hole in a sheet [18] is approximately equal to the value of K for a free surface crack multiplied by the stress concentration factor for the circular hole. As the crack deepens it runs out of the area effected by the stress concentration, and the K calculation can be based upon a crack length larger than the actual crack size only by the diameter of the hole.

A similar approach was taken in this study. The solution suggested in Ref. 4 is the only known approximation for the stress-intensity factor K at fillet weld toes. There are obvious differences in the stiffener details evaluated in this study and the welded cruciforms examined by Frank. In the cruciform joint a half tunnel crack was assumed at the weld toe together with a plate stress condition. Symmetry was also considered with plates attached to both surfaces. At the stiffener

details semi-elliptical cracks were observed. In addition, the stiffener was only attached to one side of the web or flange plate.

Two solutions were used to describe the stress-intensity factor at the fillet weld toes on the web or flange. One modified the solution obtained for a tunnel crack to reflect the semi-elliptical surface cracks. The decay polynomial obtained by Frank was assumed to describe the weld geometry effect and its decay with increasing crack depth. This yielded

$$K_T(\tfrac{a}{t}) = K_T[1 - 3.215\tfrac{a}{t} + 7.897(\tfrac{a}{t})^2 - 9.288(\tfrac{a}{t})^3 + 4.086(\tfrac{a}{t})^4] \tag{9}$$

A second decay characteristic was also examined [2]. This assumed the geometry correction function to decrease parabolically from a maximum of K_T with an infinitesimal crack, to no effect at a depth equal to the weld size. The relationship was assumed and had the following form:

for $0 < a \leq w$:

$$K_T(\tfrac{a}{t}) = K_T - 2(K_T - 1)\frac{a}{w} + (K_T - 1)(\tfrac{a}{w})^2 \tag{10}$$

and for $a \geq w$: $\quad K_T(\tfrac{a}{t}) = 1.0$

where w is the weld size.

The stress intensity factor for part-through cracks at fillet weld toes is then given by:

$$K = \frac{1 + 0.12\,(1 - \frac{a}{b})}{\Phi_o} K_T(\tfrac{a}{t})\,\sigma\sqrt{\pi a}\,\sqrt{\sec\frac{\pi a}{2t}} \tag{11}$$

where $K_T(\frac{a}{t})$ is a magnification factor which accounts for the stress raising effect of the fillet weld; a is the crack depth, and t is the thickness of the plate in which the crack is growing.

Equation 9 describes the correction function for the weld geometry in terms of the ratio a/t; it is independent of the weld size, w except for its effect on K_T. The decay characteristic given by Eq. 10 is written in terms of the ratio a/w, crack size to weld size, in an attempt to better account for variation in geometries, such as may occur when stiffeners are connected to flanges by fillet welds where the difference between t and w is substantial.

Both decay characteristics are useful when evaluating crack propagation at welded structural details where crack growth occurs at the weld termination. Equation 9 and 10 are compared in Fig. 14 for a girder with a ½ inch (12.7 mm) flange and a stiffener attached with ¼ inch (5 mm) fillet welds.

Equations 9 and 10 provide about the same estimate of stress concentration factor in the region of critical crack size. Equation 10 provides simplicity in estimating K and appears to be applicable to a wider range of plate thickness.

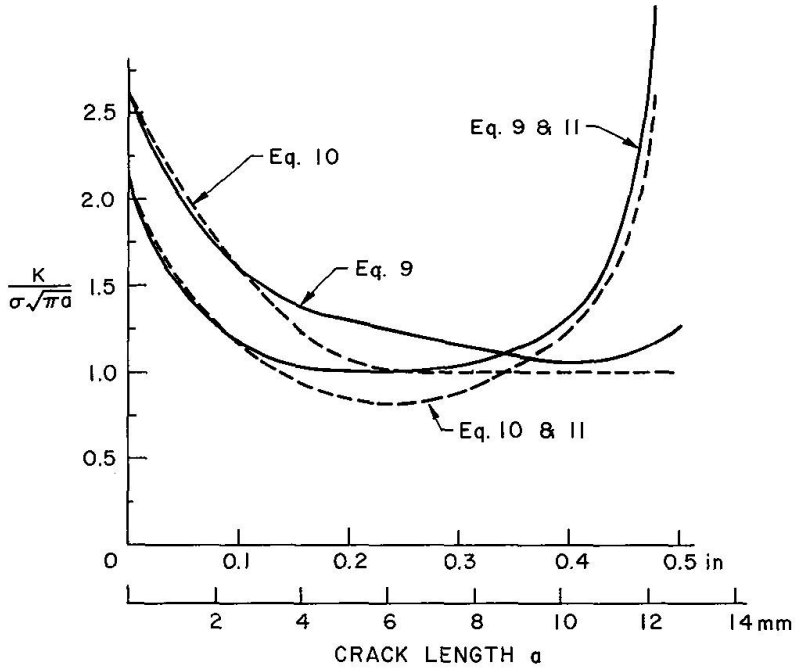

Fig. 14. Change in Stress Intensity Factor at Fillet Weld Toe with Crack Size.

Analysis of Crack Growth at Stiffeners

Equations 2, 6 and 11 were used to evaluate the crack propagation through the web and flange of the stiffener details. Since all crack were observed to grow perpendicular to the principal stress, only Mode I crack growth was considered as there was no evidence of other modes of crack growth. Before carrying out the analysis, the theoretical stress concentration factor K_T at the fillet weld toe was determined using a finite element solution. The results are tabulated in Table 1. The weld and stiffener geometry were found to have only a local concentration effect on the stress field.

The nominal stress range at stiffeners welded to the web alone was taken as the principal stress range at the end of the stiffener-to-web weld. The nominal bending stress range at the stiffener-to-flange weld was used for stiffeners welded to the web and flange.

A family of curves depicting the relationship between initial crack sizes and fatigue life for the stress range levels of this study were constructed. These curves are plotted in Figs. 15, 16 and 17 for the two types of stiffeners. The final crack sizes correspond to the values of plate thickness listed in Table 1. The points on the curves correspond to the observed fatigue lives of beams with stiffeners which experienced crack propagation through the web or flange thickness at the weld toe. For stiffeners welded to the web alone this corresponded to about 80% of the total life. For stiffeners welded to flange and web the failure life was used.

Table 1. Data for Analysis of Propagation of Part-Through Cracks

Specimen	Plate Thickness in. (mm)	Stiffener Thickness in. (mm)	Weld Size in. (mm)	Stress Concentration Factor K_T	Stress Range at Detail ksi (kN/mm²)			
					in. (mm)	in. (mm)	in. (mm)	in. (mm)
Stiffeners Welded to Web								
Beam	9/32(7.1)	9/32(7.1)	1/4(6.4)	2.20	14.8(10.2)	19.8(13.7)	24.7(17.0)	29.7(20.5)
Girder	1/4(6.4)	1/4(6.4)	1/4(6.4)	2.12	16.1(11.1)	21.5(14.8)	26.9(18.6)	
Stiffeners Welded to Flange								
Beam	3/8(9.5)	9/32(7.1)	1/4(6.4)	2.42	14.4(9.4)	19.2(13.3)	23.9(16.5)	28.7(19.8)
Girder	1/2(12.7)	1/4(6.4)	1/4(6.4)	2.64	13.8(9.5)	18.4(12.7)	22.9(15.8)	

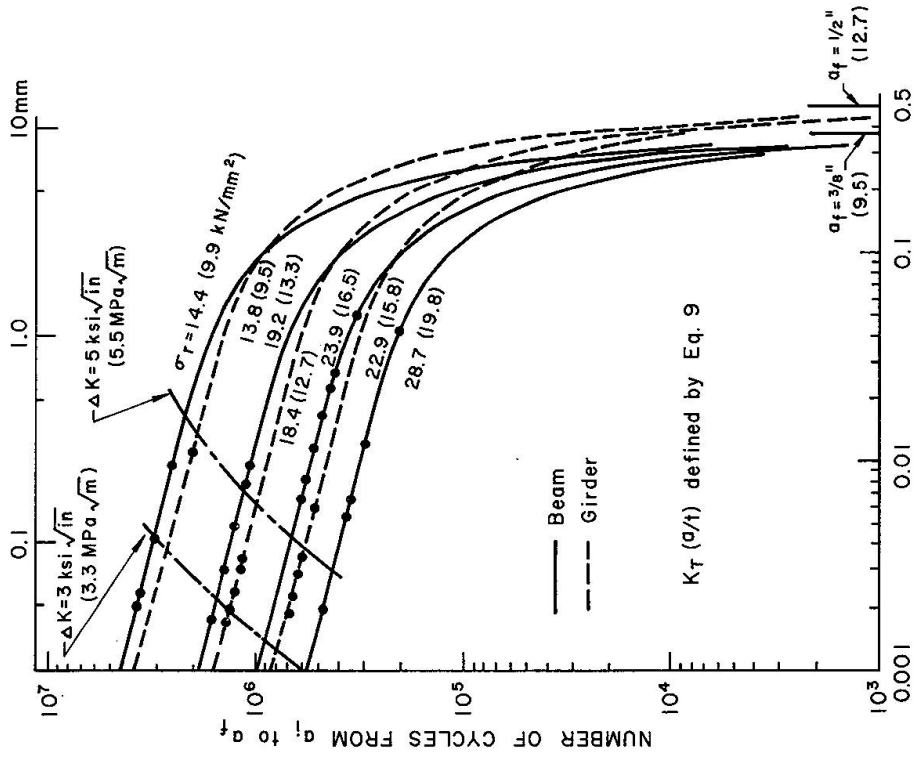

Fig. 16. Propagation of a Part-Through Crack at the Stiffener-to-Flange Connection Using Eq. 9.

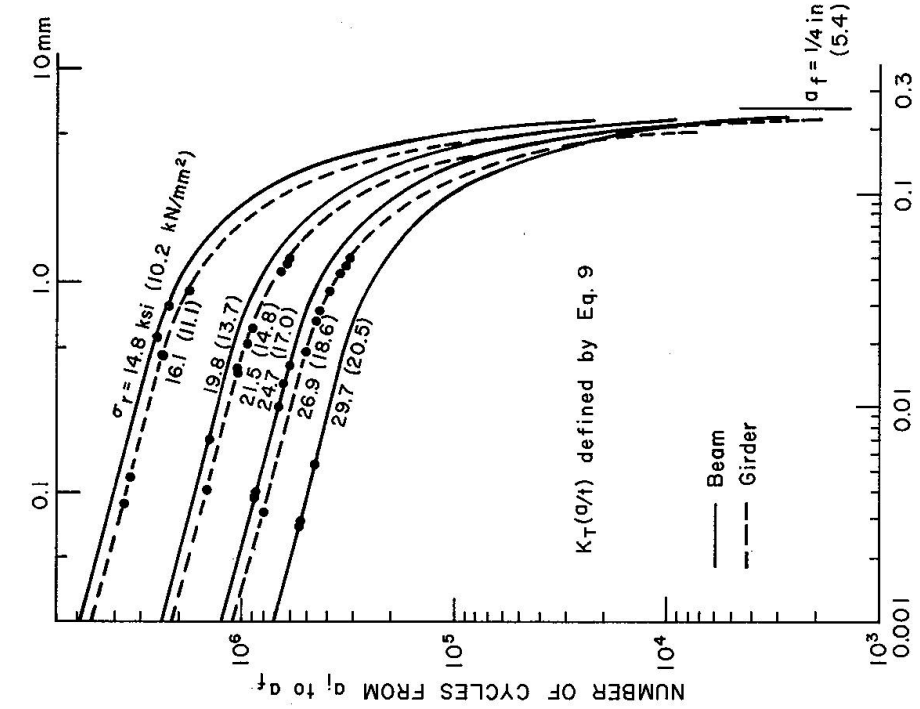

Fig. 15. Propagation of a Part-Through Crack at Stiffeners Attached to the Web Alone.

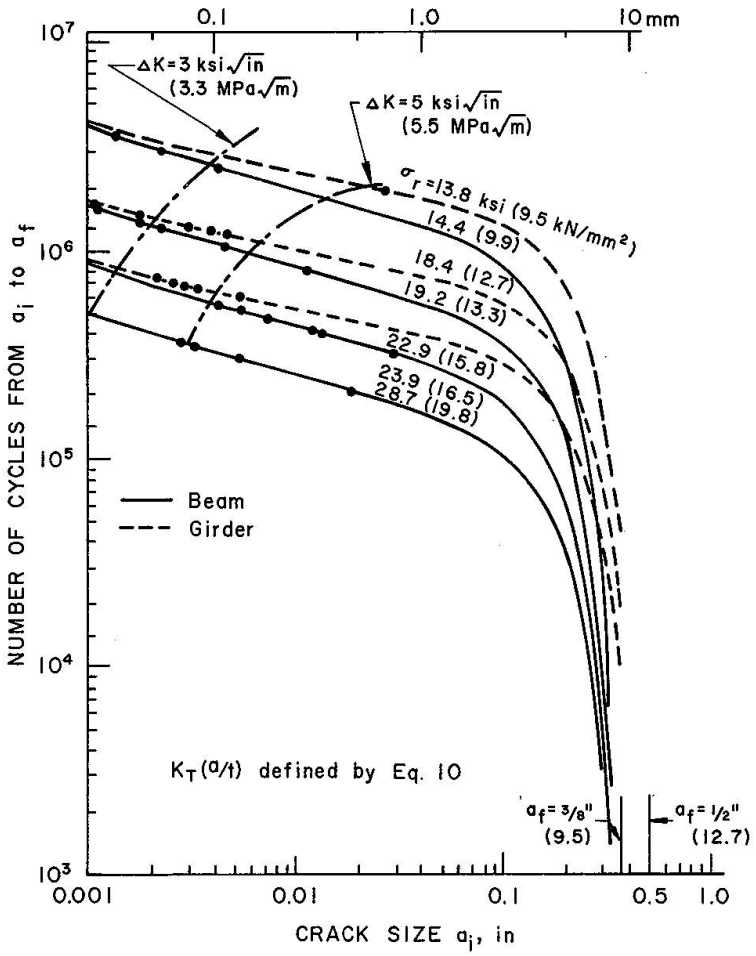

Fig. 17. Propagation of a Part-Through Crack at the Stiffener-to-Flange Connection Using Eq. 10.

Both Eqs. 9 and 10 were used to estimate the stress-intensity factor at the toe of stiffeners welded to the web and flange. A comparison of Figs. 16 and 17 shows the effect of the different stress-intensity estimates. The crack propagation analysis yields a set of curves dependent on the stress range level and the initial crack size. Both analysis agree well with the test data from beams and girders. The predicted curves are in an ordered arrangement when Eq. 10 is used. Equation 9 provides curves that are not in sequence with the stress range levels.

The observed fatigue lives correspond to initial crack sizes which are within the range of weld flaws reported in the literature [3, 5]. The average initial crack size is about 0.003 in.

The solution of Eq. 2 can also be used to construct stress range – cycle life (*S-N*) relationships for various initial crack sizes. This was done for the stiffener welded to the web and flange since nearly all the fatigue life was consumed when the crack propagated through the flange thickness. The results are shown in Fig. 18 for crack sizes of 0.001 in. (0.025 mm), 0.003 in. (0.1 mm), and 0.020 in. (0.5 mm). The relationship derived for an initial crack size of 0.003 in. (0.1 mm) is directly comparable to the mean fatigue strength; and the predicted relationship for an initial crack size of 0.020 in. (0.5 mm) provides good agreement with the lower bound of the test

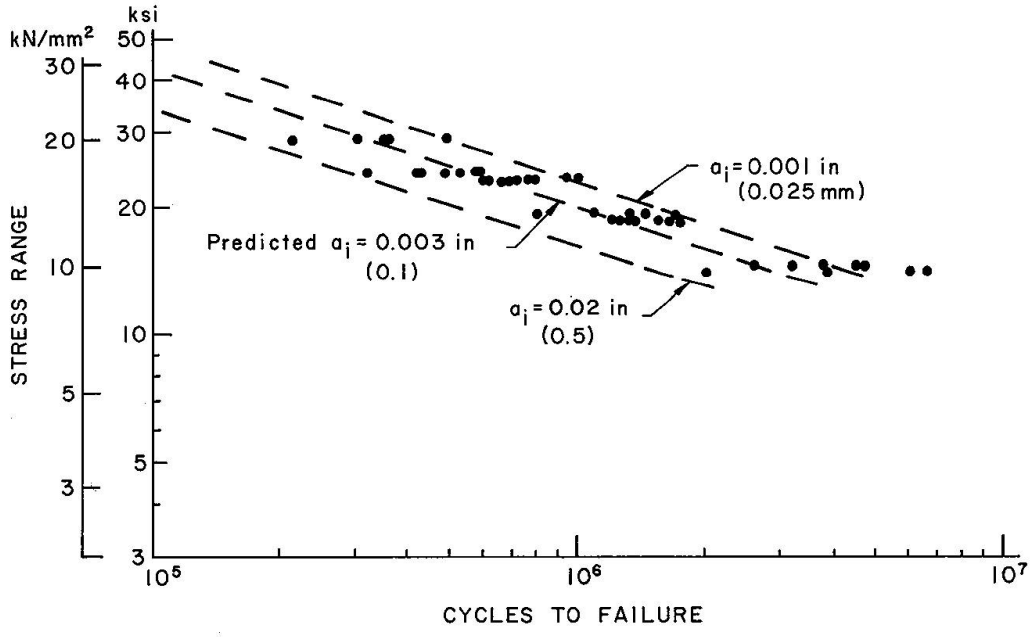

Fig. 18. Comparison of Predicted Fatigue Life with Test Data for Stiffeners Welded to Web and Flange.

data. Only test data at the 13.8 ksi (9.5 kN/mm^2) stress range level exceeded the predicted life. As can be seen in Figs. 16 and 17, specimens with average or below average initial crack sizes may be at or below the fatigue crack growth threshold. The probability of this happening increases with a decreasing stress range.

The results obtained from the analysis indicate that the proposed mathematical model for propagation of a part-through crack at the weld toe of stiffeners is in good agreement with the observed fatigue behavior.

Conclusions and Application

Fracture mechanics was used to analyze the fatigue behavior of transverse stiffeners welded to the web alone or to the web and flanges. The analysis considered crack propagation of a crack through the thickness of the web and the flange. This showed that 80% of the total number of cycles to failure at web stiffeners and 96% at web-flange stiffeners were consumed during this stage of growth.

The main conclusions are:

1. The fatigue cracks initiated from weld discontinuities at the fillet weld toes. They retained the approximate shape of a semi-ellipse as they propagated through the plate thickness.
2. The stress-intensity factor for a part-through crack in a flat plate can be used in conjuction with a correction function accounting for the stress concentration effect of the weld geometry to describe the stress condition at the leading edge of the crack.

3. Integration of the differential equation of crack growth revealed that the mean fatigue life corresponded to an equivalent initial crack depth of about 0.003 in. (0.1 mm).
4. The scatter in the test data can be associated with the variation of the initial crack sizes.
5. At the lowest stress range, to which the test specimens were subjected, and an equivalent mean initial crack size $a_i = 0.003$ in. (0.1 mm), crack growth appeared to occur slightly below the threshold levels reported in the literature.
6. 98% of the number of cycles required to propagate the part-through crack across the plate thickness elapsed as the leading edge of the crack advanced to a depth of 0.75 t.

Application: Since most of the details fatigue life was consumed growing a part-through crack, the study emphasizes the need for properly designing a structure to assure adequate performance without premature failure. There is little likelihood of detecting part-through cracks before failure or in fabricating smaller discontinuities. The paper shows that design for a proper stress range level and adequately assessing the loading of structures are the most realistic and reliable means of assuring the desired service life.

The method also provides a means to evaluate the formation and propagation of cracks in other types of welded built-up structures.

Notation

a	crack size, minor half-axis for semi elliptical crack.
a_f	final crack size.
a_i	initial crack size.
B_1, B_2	regression coefficients.
b	major half-axis for semi-elliptical crack.
C	coefficient in crack growth equation.
da/dN	rate of crack growth, inch/cycle.
G	constant in regression equation ($= 10^{B_1}$).
K	stress-intensity factor.
K_T	theoretical stress concentration factor.
N	number of applied stress cycles.
n	exponent in crack growth equation.
t	plate thickness.
Φ_o	complete elliptical integral of the second kind.
ΔK	stress-intensity factor range.
σ	stress.
σ_r	stress range.

Acknowledgments

The research reported herein was performed under the National Cooperative Highway Research Project 12-7 at Fritz Engineering Laboratory, Department of Civil Engineering, Lehigh University, Bethlehem, Pennsylvania.

The opinions and findings expressed or implied in this paper are those of the writers. They are not necessarily those of the Highway Research Board, the National Academy of Science, the Bureau of Public Roads, the American Association of State Highway Officials, nor of the individual states participating in the National Cooperative Highway Research Program.

References

1. FISHER, J.W., ALBRECHT, P., YEN, B.T., KLINGERMAN, D.J., and MCNAMEE, B.M.: Effect of Weldments on the Fatigue Strength of Steel Beams with Transverse Stiffeners and Attachments. NCHRP Report, No. 147, Highway Research Board, National Academy of Sciences — National Research Council, Washington, D.C., 1974.
2. ALBRECHT, P.: Fatigue Strength of Welded Beams with Stiffeners. Ph. Dissertation, Lehigh University, Bethlehem, Pennsylvania, July 1972.
3. SIGNES, E.G., BAKER, R.G., HARRISON, J.D., and BURDEKIN, F.M.: Factors Affecting the Fatigue Strength of Welded High-Strength Steels. British Welding Journal, February 1967.
4. FRANK, K.H.: The Fatigue Strength of Fillet Welded Connections. Ph. D. Dissertation, Lehigh University, Bethlehem, Pennsylvania, 1971.
5. WATKINSON, F., BODGER, P.H., and HARRISON, J.D.: The Fatigue Strength of Welded Joints in High-Strength Steels and Methods for its Improvement. Proceedings, Fatigue of Welded Structures Conference, the Welding Institute, Brighton, England, July 1970.
6. PARIS, P.D., GOMEZ, M.P., and ANDERSON, W.E.: A Rational Analytical Theory of Fatigue. The Trend in Engineering, University of Washington, Vol. 13, No. 1, January 1961.
7. IRWIN, G.R.: Analysis of Stresses and Strains Near the End of a Crack Traversing a Plate. Transactions, ASME, Series E, Vol. 24, No. 3, September 1957.
8. FISHER, J.W., FRANK, K.H., HIRT, M.A., and MCNAMEE, B.M.: Effect of Weldments on the Fatigue Strength of Steel Beams. NCHRP Report No. 102, Highway Research Board, National Academy of Sciences — National Research Council, Washington, D.C., 1970.
9. BARSOM, J.M.: Fatigue-Crack Propagation in Steel of Various Yield Strengths, U.S. Steel Corp., Applied Research Laboratory, Monroeville, Pennsylvania, 1971.
10. PARIS, P.C.: Testing for Very Slow Growth of Fatigue Cracks. Closed Loop, MTS System Corp., Vol. 2, No. 5, 1970.
11. CROOKER, T.W., and LANGE, E.A.: How Yield Strength and Fracture Toughness Considerations can Influence Fatigue Design Procedures for Structural Steel. Welding Research Supplement, Vol. 49, No. 10, October 1970.
12. MADDOX, S.J.: Fatigue Crack Propagation in Weld Metal and Heat Affected Zone Material. Members' Report No. E/29/69, The Welding Institute, England, December 1969.
13. HARRISON, J.D.: An Analysis of Data of Non-Propagating Fatigue Cracks on a Fracture Mechanics Basis, British Welding Journal, Vol. 2, No. 3, March 1970.
14. HIRT, M.A., and FISHER, J.W.: Fatigue Crack Growth in Welded Beams. To be published in the Journal of Engineering Fracture Mechanics.
15. FRANK, K.H., and FISHER, J.W.: The Fatigue Strength of Welded Coverplated Beams. Fritz Engineering Laboratory Report No. 334.1, Lehigh University, Bethlehem, Pennsylvania, March 1969.
16. IRWIN, G.R.: Crack Extension Force for a Part-Through Crack in a Plate. Transactions, ASME, Series E. Vol. 29, December 1962.

17. IRWIN, G.R., LIEBOWITZ, H., and PARIS, P.D.: A Mystery of Fracture Mechanics. Engineering Fracture Mechanics, Vol. 1, 1968.
18. PARIS, P.D., and SIH, G.C.: Stress Analysis of Cracks. ASTM Special Technical Publication, No. 381, 1970.
19. MADDOX, S.J.: Calculating the Fatigue Strength of a Welded Joint Using Fracture Mechanics. Metal Construction, Vol. 2, No. 8, August 1970.

Summary

The fatigue behavior of welded beams with transverse stiffeners was determined experimentally by carrying out 52 tests on 350 mm and 970 mm deep beams. Initiation of fatigue cracks from defects at weld toes and their propagation through characteristic stages of growth to failure of the beams are described. Fracture mechanics concepts are applied to the stage of growth as a part-through crack during which most of the fatigue life is spent, in order to relate the observed life to the crack size.

Résumé

La résistance à la fatigue des poutrelles d'acier de 350 mm et 970 mm de hauteur pourvues de raidisseurs soudés a été déterminée à l'aide de 52 essais. L'article montre que les fissures commencent le long des soudures et se propagent en plusieurs stages caractéristiques. En utilisant les méthodes d'analyse de la mécanique de rupture, on établit la relation entre le nombre de charges appliquées et les dimensions de la fissure pendant le premier stage, qui est le plus important.

Zusammenfassung

Die Ermüdungsfestigkeit geschweisster Stahlbalken mit Querversteifungen wurde experimentell anhand von 52 Versuchen an Balken von 350×970 mm bestimmt. Der Artikel zeigt, dass die Risse entlang den Schweisstellen beginnen und sich auf mehrere charakteristische Stadien ausbreiten. Unter Verwertung der Berechnungsmethode über die Mechanik des Bruchvorganges wird die Beziehung zwischen der Zahl der angewandten Lasten und den Abmessungen des Risses während der ersten Phase, welche die wichtigste ist, aufgestellt.